

Amination of polypropylene-g-(maleic anhydride) using reactive extrusion

Ian P. Kay | Julie M. Goddard 

Department of Food Science, Cornell University, Ithaca, New York, USA

Correspondence

Julie M. Goddard, Department of Food Science, Cornell University, Ithaca, New York 14853, USA.
Email: goddard@cornell.edu

Funding information

National Institute of Food and Agriculture, Grant/Award Number: 2019-68015-29230; National Science Foundation, Grant/Award Number: DMR-1719875

Abstract

We report synthesis of a radical scavenging aminated thermoplastic polymer through reactive extrusion of polyethyleneimine (PEI) with a polypropylene and polypropylene-graft-maleic anhydride (PP-g-MA) meltblend. The reaction was confirmed using acid orange 7 (AO7) amine density assay, toluidine blue O (TBO) carboxylic acid density assay, Fourier transform infrared spectroscopy (FTIR), and a migration assay. FTIR spectra revealed a reduction of the asymmetric stretching of the maleic anhydride (MA) carbonyl group at 1777 cm^{-1} and the emergence of the maleimide carbonyl peak at 1702 cm^{-1} . AO7 supported surface orientation of grafted amine groups by introduction of 7.22 nmol cm^{-2} primary amines, corresponding to the reduction of surface carboxylic acids quantified by TBO from $12.46\text{ nmol cm}^{-2}$ to 0.43 nmol cm^{-2} . After incubation (40°C , 10 days) in ethanol, acetic acid, and water, $< 0.1\text{ mg cm}^{-2}$ PEI migrated from the materials, supporting the covalent nature of the grafting. Antioxidant activity was demonstrated exhibiting 5.90 and $4.31\text{ nmol Trolox}_{\text{eq}}\text{ cm}^{-2}$ in aqueous and organic environments, respectively. Results indicate a successful condensation reaction during reactive extrusion, producing an aminated thermoplastic polymer with antioxidant activity for target applications such as food packaging, wastewater treatment, carbon capture, and others.

KEY WORDS

aminated polymer, antioxidant, functional polymer, radical scavenging, reactive extrusion

1 | INTRODUCTION

Amine functionalized polymers have been reported for applications in water treatment,¹ carbon capture,² biomedicine,^{3,4} surface modifications⁵ and more. They have been shown potential as inexpensive and effective adsorbents to remove impurities from wastewater⁶ as well as carbon dioxide capture from industrial gas streams.⁷ In medicine, amine functionalized polymers have been explored as drug delivery systems with a stronger and more targeted immune response and as implanted devices with increased biocompatibility and adhesion.⁸

Polyethyleneimine (PEI) is an amine rich polycation that is available in both linear and branched forms at varying molecular weights and thus has been explored as an aminating reagent for synthesis of aminated polymers. Previous studies with PEI have demonstrated its metal chelating,⁹ antibacterial,¹⁰ and antioxidant properties¹¹; however, its reported cytotoxic effects on living organisms¹² necessitate that it be covalently bound to a polymer so that its beneficial properties can be realized without the introduction of toxic side effects.

Current approaches to synthesizing amine rich polymers often leverage wet chemistry techniques either in

bulk polymer modification or post synthesis surface modifications.^{13,14} While these methods are effective in a lab setting, they can be expensive, time consuming, and rely on significant solvent use and often hazardous chemicals, limiting their translation to greener industrial scale production. In contrast, reactive extrusion is a solvent-free, continuous process used commercially to synthesize and modify polymeric materials.¹⁵ For example, Wang et al. produced branched polypropylene (PP) by reacting isotactic PP with the polyfunctional monomer pentaerythritol triacrylate,¹⁶ while Raquez maleated thermoplastic starch using maleic anhydride (MA) for improved processing and reactivity.¹⁷ Indeed, the grafting of MA onto PP is one of the most common modifications performed using reactive extrusion.¹⁵ Reactive extrusion has also been used to add active functional properties (antioxidant, antimicrobial, etc.) to polymeric materials for specific applications. Vaidya et al. was able to create a green and scalable method of grafting polycaprolactone (PCL) to chitosan using reactive extrusion for use as an antimicrobial polymer.¹⁸ Similarly, Liu et al. used reactive extrusion to create a bifunctional antimicrobial air filter by radically grafting 2,4-diamino-6-diallylamino-1,3,5-triazine (NDAM) to polypropylene and then chlorinating the grafted product.¹⁹ Whether creating a co-polymer with inherent antimicrobial properties, or grafting an intermediate that can be easily treated to add antimicrobial properties, Vaidya, Liu, and many other authors demonstrate the versatility of reactive extrusion for adding functional properties to polymers.^{15,20,21} Several reports have been published on using reactive extrusion for grafting amine groups onto MA groups in the melt. In one report, Létoffé et al. reacted polyether triamine with polypropylene-g-maleic anhydride (PP-g-MA) to improve mechanical properties (via crosslinking) and adhesion to metal surfaces.²² In another, Cao et al. reacted ethylenediamine with PP-g-MA with improved mechanical properties, demonstrating the influence of supercritical carbon dioxide in the processibility and final mechanical properties of the resulting crosslinked polymer.²³ Others have reported additional approaches to synthesize specific chemistries of thermoplastics modified by reactive extrusion of low molecular weight diamines with MA functionalized polypropylene.²⁴⁻²⁶ Our group has used reactive extrusion to graft the nitrilotriacetic acid to polylactic acid (PLA)²⁷ for an antioxidant active packaging application, curcumin to polypropylene²⁸ for both antioxidant and intelligent color changing properties, and polylysine to polypropylene to impart antimicrobial activity.²⁹ These reports demonstrate the potential of reactive extrusion in reducing solvent use and the number of steps needed to functionalize polymers for targeted applications, positioning reactive extrusion to be a more translatable, and green

polymer modification process than wet chemical approaches.

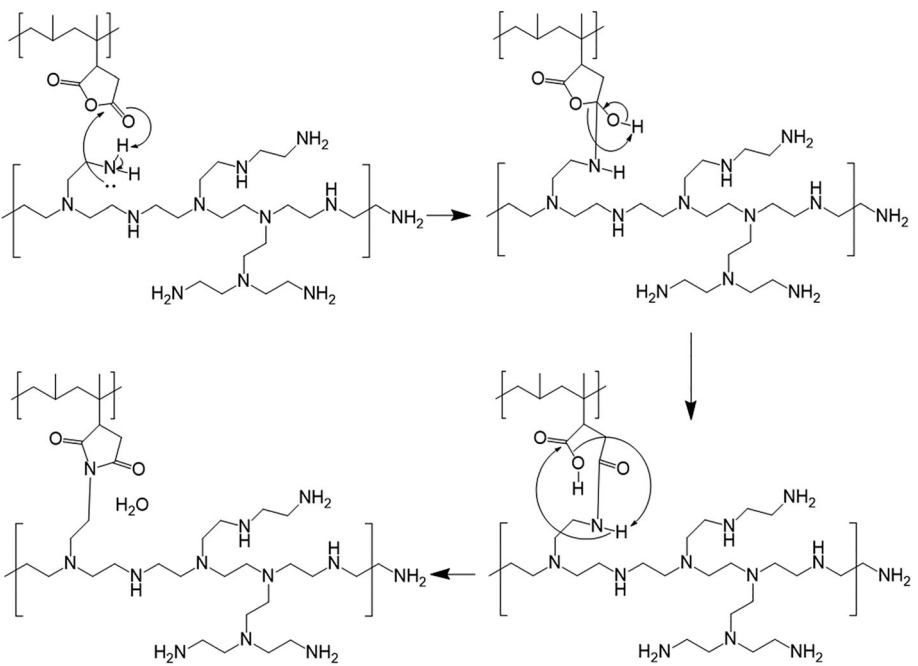
While several reports have been published on using reactive extrusion to introduce specific functional properties (e.g. antimicrobial, antioxidant), and others have been reported specific to amination of maleated thermoplastics with di- and triamine small molecules for improved mechanical and adhesion properties, there remains an opportunity to investigate amination of maleated thermoplastic by highly aminated polymers to introduce surface active functional groups for targeted applications. The current study aims to graft branched PEI onto polypropylene-*graft*-maleic anhydride (PP-g-MA) blended with native polypropylene using a condensation reaction in a twin-screw extruder to produce (PP-g-MA)-g-PEI, an aminated polymer with potential application in active food packaging, carbon capture, filtration, biosensors, and more. Branched PEI contains a spreading network of primary amines available to react with the anhydride groups of PP-g-MA, forming a maleimide at the grafting site. Covalent binding of PEI to PP-g-MA with introduction of surface oriented amine groups was confirmed through surface chemistry characterization and migration assays. The antioxidant activity of the (PP-g-MA)-g-PEI introduced by PEI was characterized using Trolox equivalence assays.

2 | EXPERIMENTAL

2.1 | Materials

2,2-diphenyl-1-picrylhydrazyl (DPPH), glacial acetic acid, hydrochloric acid (trace-metal grade), (\pm)-6-hydroxy-2,5,7,8-tetramethylchromane-2-carboxylic acid (Trolox, 97%), branched PEI (Mw \sim 25,000), PP-g-MA, MW \sim 9100 pellets (MA 8–10 wt%), potassium persulfate (\geq 99%), sodium phosphate dibasic heptahydrate, sodium phosphate monobasic monohydrate, and toluidine blue O (TBO) dye were purchased from Millipore Sigma (Burlington, MA). 2,2'-Azino-bis(3-ethylbenzothiazoline-6-sulfonic acid) diammonium salt (ABTS, 98%) and sodium hydroxide were purchased from Fisher Scientific (Fair Lawn, NJ). Ethanol (200 proof) was obtained from Decon Laboratories (King of Prussia, PA). Orange II (AO7) was obtained from Acros Organics (New Jersey, USA). Deuterium Oxide (99.9%) was obtained from Cambridge Isotope Laboratories (Andover, MA). Isotactic polypropylene pellets (PP) were obtained from Scientific Polymer (Ontario, NY). Grades U, E, and EX purge for the extruder were generously provided by Asahi Kasei Asaclean Americas (Parsippany, NJ). Kapton films were purchased from Cole-Parmer (Vernon Hills, IL). All

SCHEME 1 Proposed condensation reaction between the primary amine groups of PEI and anhydride groups of PP-g-MA resulting in final aminated polymer (PP-g-MAX)-g-PEIY, in which X represents weight percent of MA in PP-g-MA / PP masterbatch blends and Y represents weight percent of PEI in final polymer. MA, maleic anhydride; PEI, polyethylenimine.



reagents were used as received without further purification unless stated otherwise.

2.2 | Extrusion of polypropylene and polypropylene-g-maleic anhydride blends

PP were mixed then melt-blended with PP-g-MA pellets to produce compatibilized masterbatch blends of MA content of 1% and 3% by weight (PP-g-MA1 & PP-g-MA3, respectively). Masterbatches were extruded at 200 rpm through a Process 11 Parallel Twin Extruder (Thermo ScientificTM) fit with a 1 mm die with the temperature profile for zones 2–8 and the die of 140, 165, 165, 175, 175, 185, 185, 190°C respectively. The resultant extrudate was then pelletized in a Process 11 VariCut Pelletizer (Thermo ScientificTM) at the L1 position for a final length of 0.5 mm and then stored over calcium sulfate desiccant for at least 24 h prior to further use.

2.3 | Synthesis of aminated polypropylene-g-maleic anhydride films (PP-g-MAX)-g-PEIY

Branched PEI was grafted to the polypropylene-g-maleic anhydride blends (PP-g-MA1 & PP-g-MA3) through a condensation reaction between the primary amines of the PEI and the anhydride groups of PP-g-MA blends resulting in final aminated polymer (PP-g-MAX)-g-PEIY, in which X represents weight percent of MA in PP-g-MA / PP masterbatch blends and Y represents weight percent of PEI in final polymer (Scheme 1). PP-g-MA1 and PP-g-MA3 were

first mixed with PEI (1, 3, or 5% by weight) and then dried in an oven at 80°C for 4 h to reduce the presence of water during reaction. Dried mixtures were then extruded in a Process 11 Parallel Twin Extruder (Thermo ScientificTM) at 250 rpm fit with a 1 mm die with the temperature profile for zones 2–8 and the die of 140, 175, 175, 190, 190, 190, 190, and 200°C, respectively. The aminated product was then pelletized in a Process 11 VariCut Pelletizer (Thermo ScientificTM) at the L1 position for a final length of 0.5 mm and then stored over calcium sulfate desiccant. Films were prepared by pressing 2 g of each extrudate between 5 mil Kapton films using a Carver hot press (Wabash, IN). Pellets were arranged in a compact circle between the Kapton films and allowed to melt between the platens at 180°C for 5 min before pressing at 2000 pound force for 2 min. The films were then washed by submerging in excess absolute ethanol with stirring for 4 h at 20°C, rinsed under distilled water to remove residual ethanol, then dried with filtered compressed air and stored over calcium sulfate desiccant prior to characterization. A 4 h ethanol washing time at 20°C was determined to be sufficient time to remove surface contaminations introduced by hot pressing and unreacted reagents but well under standard migration testing conditions (e.g. 10 days at 40°C), thus sufficient for film cleaning prior to subsequent surface analytical testing.

2.4 | Surface chemistry characterization of (PP-g-MAX)-g-PEIY films

Primary amine density on the surface of the (PP-g-MAX)-g-PEIY films was quantified using the acid orange seven (AO7)

dye assay in which AO7 dye is reported to complex in a 1:1 molar ratio with available primary amine groups.^{30–32} Film coupons ($2 \times 1 \text{ cm}^2$) were incubated for 3 h in excess 1 mM AO7 dye solution adjusted to pH 3 with 1 M HCl. After incubation, films were washed in pH 3 water to remove any unbound dye before desorption in 3 mL of water adjusted to pH 12 by 1 M NaOH for 15 min. Absorbance of a 250 μL aliquot of desorbed dye solution was then measured at 455 nm on a Synergy Neo2 Hybrid Multi-Mode Reader (BioTek Instruments, Winooski, VT) and compared with a standard curve of AO7 in water adjusted to pH 12 by 1 M NaOH to quantify the number of primary amines on the surface of each sample in units of nmol primary amines per cm^2 with films prepared from PP and PP-g-MAX as controls.

Carboxylic acid density was measured using the TBO dye assay as previously described in which TBO dye is reported to complex in a 1:1 molar ratio with available carboxylic acid groups.^{31,33,34} Film coupons ($2 \times 1 \text{ cm}^2$) were incubated for 3 h in excess 0.5 mM TBO solution adjusted to pH 10 by 1 M NaOH. After incubation, films were washed three times in water adjusted to pH 10 using 1 M NaOH to remove any unbound dye. Complexed dye was then desorbed in 3 mL of 50% glacial acetic acid for 15 min. The absorbance of the desorbed solution was then measured at 562 nm and compared with a standard curve of the TBO dye in 50% acetic acid to quantify the number of carboxylic acids on the surface of each sample in units of nmol of carboxylic acid per cm^2 with films prepared from PP and PP-g-MAX as controls.

Attenuated total reflectance Fourier transformative infrared spectroscopy (ATR-FTIR, Shimadzu Scientific Instruments, Inc., Kyoto Japan) was used to further characterize the surface chemistry of the (PP-g-MAX)-g-PEI5 films. Absorbance spectra were collected using the Happ-Genzel function with 32 scan resolution and analyzed to confirm the presence of amines, amide bonds, and the formation of the maleimide post reaction. Spectra were collected on three different spots on three separate $2 \times 1 \text{ cm}^2$ coupons prepared from each of two biological replicates directly after hot pressing to reduce the likelihood of any interference with the films surface chemistry, with films prepared from PP and PP-g-MAX as controls. A random number generator was then used to select one spectra of each sample for reporting. Spectra were analyzed using the OriginPro 2022B software (Origin Labs Corporation) and the KnowItAll Informatics Systems program (John Wiley and Sons, 2023).

2.5 | Nonmigratory behavior of (PP-g-MAX)-g-PEI5 films

Migration assays for (PP-g-MAX)-g-PEI5 films were conducted in four solvents of varying proticity and polarity,

defined by European Union and United States Food and Drug Administration regulations for assessing the safety of food contact materials. Absolute ethanol was used to represent potential migration in contact with high fatty foods, 10% ethanol and 3% acetic acid was used to represent potential migration in acidic foods, and water to represent potential migration in aqueous foods.^{35,36} Film coupons ($2 \times 1 \text{ cm}^2$) were incubated in 10 mL of each solvent for 10 days at 40°C. After incubation, the films were removed from the solvents and solvents were evaporated to dryness over Lab Armor beads. Leached PEI was dissolved in 0.5 mL of deuterium oxide for NMR spectroscopy. H^1 spectra were obtained using four scans on a 500 MHz Bruker NMR with an acquisition time of 3.2768 s, a 10 KHz spectral width, a 30 s relaxation delay, and a 90° excitation pulse. Results were compared with a standard curve of PEI in deuterium oxide and expressed as mg PEI / cm^3 . To determine if nonmigratory behavior of (PP-g-MAX)-g-PEI5 films was a result of noncovalent compatibilization induced during extrusion or covalent binding of primary amines to MA groups, a new set of control films (PP-PEI5) were prepared and analyzed in the migration assay. PP-PEI5 was prepared by extruding 5 wt% PEI in PP in the absence of PP-g-MA under the same extrusion conditions as in preparation of (PP-g-MAX)-g-PEI5.

2.6 | Radical scavenging capacity of (PP-g-MAX)-g-PEI5 films

Radical scavenging capacities of PP and PP-g-MAX (control) and (PP-g-MAX)-g-PEI5 films were quantified using the ABTS and DPPH Trolox equivalency (Trolox_{eq}) assays, which characterize radical scavenging capacity in aqueous and organic environments, respectively. Trolox equivalency assays were performed after 1, 2, 4, 6, and 24 h incubation to characterize the radical scavenging capacity over time.

For the ABTS assay, sodium phosphate dibasic heptahydrate and sodium phosphate monobasic monohydrate were used to prepare 4 mM phosphate buffers at pH 7.4. An ABTS radical stock solution was made by reacting equal volumes of 7 mM ABTS with 2.45 mM potassium persulfate for 16 h at $17 \pm 1^\circ\text{C}$ in the dark. The ABTS radical stock solution was then adjusted with buffer to an absorbance of 0.90 ± 0.05 at 734 nm using a Synergy Neo2 Hybrid Multi-Mode Reader (BioTek Instruments, Winooski, VT). Film coupons ($1 \times 1 \text{ cm}^2$) of PP and PP-g-MAX (control) and (PP-g-MAX)-g-PEI5 were incubated in 500 μL of the adjusted ABTS solution and 500 μL of phosphate buffer in a 24 well plate for 10 min in the dark at 30°C on an orbital shaker at 80 rpm. After incubation, a 250 μL aliquot was taken, and the absorbance at 734 nm was immediately quantified. Absorbances were

compared with a Trolox standard curve prepared from a 50:50 mixture of the phosphate buffer and ABTS solution and antioxidant activity in aqueous environments was reported in nmol Trolox_{eq} per cm² film.

For the DPPH assay, a 0.1 mM solution of DPPH in absolute ethanol was prepared. Film coupons (1 × 1 cm²) of PP and PP-g-MAX (control) and (PP-g-MAX)-g-PEI5 were then incubated in 500 μL of the DPPH radical solution and 500 μL of absolute ethanol in a 24 well plate at 25°C in the dark on an orbital shaker set to 80 rpm. After incubation, a 250 μL aliquot was taken and the absorbance at 517 nm was immediately quantified. Results were compared with a Trolox standard curve in a 50:50 mixture of the phosphate buffer and DPPH solution and antioxidant activity in organic environments were reported in nmol Trolox_{eq} per cm² film.

2.7 | Surface hydrophobicity of (PP-g-MAX)-g-PEI5 films

Advancing and receding water contact angle measurements were recorded using a Attension Theta Optical Tensiometer (Biolin Scientific, Stockholm, Sweden). Contact angles were measured on three different spots of control and functionalized films by dispensing a 5 μL droplet of deionized water and recording the angle at which the baseline started to advance and then recede as the droplet increased and then decreased in size.^{31,37,38} Results are expressed as the average angle of the three spots for advancing and receding contact angle.

2.8 | Thermal properties of (PP-g-MAX)-g-PEI5 films

Differential scanning calorimetry (DSC) and Thermal gravimetric analysis (TGA) were employed to investigate the melt temperature, crystallization temperature, and degradation temperature of control and functionalized films. DSC spectra were collected using the heat, cool, heat method and results were taken from the second heating. Samples were heated to 190°C at a rate of 10°C per minute and cooled to –20°C at the same rate. For TGA, samples were heated from 0 to 600°C at a rate of 10°C per minute. Results for TGA are expressed as the temperature at which 50 wt% of the material remains.

2.9 | Statistical analysis

(PP-g-MAX)-g-PEIY was extruded in two independent biological batches on two separate days. Assays were

performed on both biological replicates. For AO7 dye assay, TBO dye assay, migration testing, ABTS and DPPH radical scavenging assays, and dynamic water contact angle significant differences were calculated using a two-way analysis of variance (ANOVA) with Tukey's honestly significant difference (HSD) multiple comparisons ($p < 0.05$) performed on GraphPad Prism 10.0.2 (Boston, MA).

3 | RESULTS AND DISCUSSION

3.1 | Synthesis of aminated polypropylene-g-maleic anhydride films ((PP-g-MAX)-g-PEIY)

Condensation reactions can be employed in reactive extrusion to synthesize polymers, alter their thermal and mechanical properties, and add functional properties for specific target applications. Examples of condensation based reactive extrusion include the polymerization of diacids with diamines to produce Nylon,¹⁵ the production of polyurethane by reacting diisocyanates and polyols,³⁹ esterification and transesterification reactions to modify starch,⁴⁰ and numerous others.^{41,42} In the present study, a catalyst- and solvent-free condensation reaction was performed to graft branched PEI onto a compatibilized blend of polypropylene with PP-g-MA using reactive extrusion. Condensation reactions between aliphatic amines and MA moieties are well studied.^{43–45} The proposed reaction mechanism is shown in Scheme 1, where the high temperature and pressure conditions in the extruder barrel facilitate a nucleophilic attack from the primary amines of PEI to the anhydride groups of PP-g-MA forming a maleimide at the grafting site.

Side reactions were mitigated by controlling the processing and reaction conditions as described by Moad et al.^{15,40,46} Mixing efficiency is critical in optimizing grafting while minimizing crosslinking and homopolymerization, two of the more prominent side reactions for the present study. To ensure proper mixing, size reduced PP-g-MA blends were mixed with PEI prior to reactive extrusion at 250 rpm. The high rotation speeds ensure the three mixing zones (3, 4, 6, and) uniformly distributed PEI throughout the melt, reducing the likelihood of crosslinking and homopolymerization. Furthermore, by controlling the temperature of the reaction and the ratio of PEI to PP-g-MA, we were able to increase the number of surface oriented primary amines, as quantified by dye assay (Figure 1). Moad et al. describes how raising the temperature and increasing the functional moiety concentration (PEI in the present study) can minimize crosslinking and homopolymerization, allowing for more free

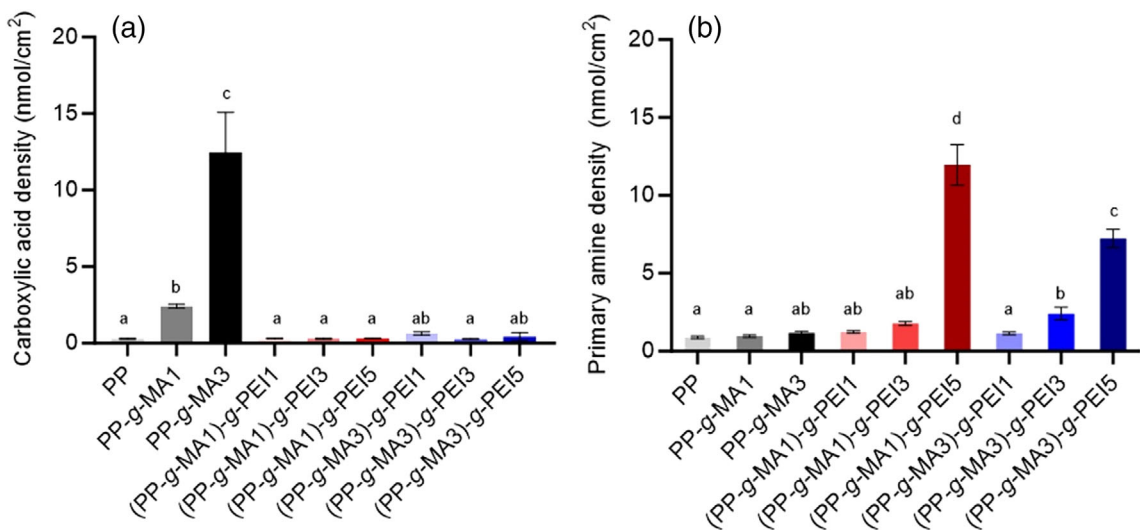


FIGURE 1 Surface characterization results for control and active films. Figure 1a shows the results from the TBO dye assay, while Figure 1b shows the AO7 dye assay. Results are displayed as the mean \pm the standard deviation ($n = 4$). Letters represent significant differences between samples. Significant differences were calculated using a two-way ANOVA with Tukey's HSD multiple comparisons ($p < 0.05$). ANOVA, analysis of variance; MA, maleic anhydride; PEI, polyethyleneimine; TBO, toluidine blue; PP, polypropylene pellets. [Color figure can be viewed at wileyonlinelibrary.com]

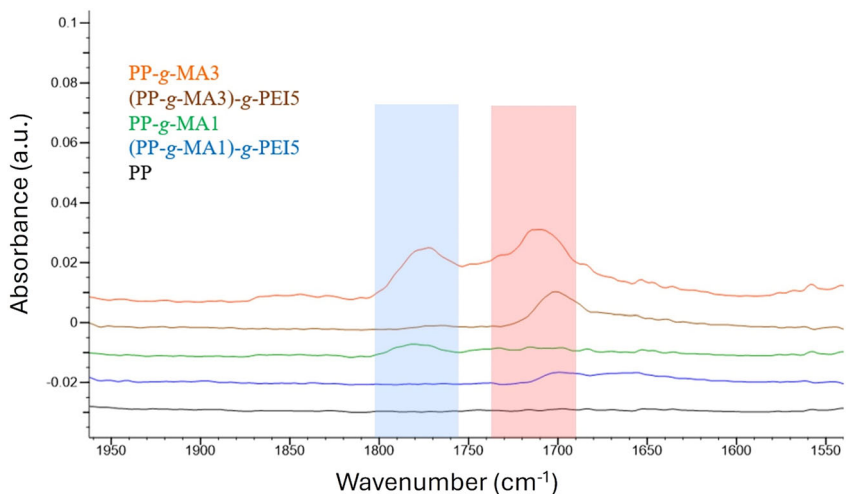


FIGURE 2 Attenuated total reflectance Fourier transform infrared spectroscopy analysis of amine functionalized and control films. The blue highlighted band (centered around $\sim 1775 \text{ cm}^{-1}$) represents the $\text{C}=\text{O}$ stretching of the carboxylic acid groups in PP-g-MA1 and PP-g-MA3 while the red highlighted band (centered around $\sim 1710 \text{ cm}^{-1}$) represents the shift of the asymmetric stretching of the maleic anhydride carbonyl in PP-g-MA3 to the stretching of the $\text{C}=\text{O}$ of the maleimide groups in (PP-g-MA3)-g-PEI5. PEI, polyethyleneimine; PP, polypropylene pellets. [Color figure can be viewed at wileyonlinelibrary.com]

primary amines throughout the polymer matrix.¹⁵ Results from the TGA thermograms for branched PEI and PP-g-MA are reported in Table S1 and were used to guide the temperature profile of the extruder zones to prevent the reactants from degrading.

3.2 | Surface chemistry characterization of (PP-g-MAX)-g-PEI5 films

Films produced from control and amine functionalized PP were analyzed for carboxylic acid and primary amine density. The TBO dye assay (Figure 1A, left) was used to determine the number of surface oriented carboxylic acid groups, while the AO7 assay (Figure 1B, right) was used

to quantify the number of surface oriented primary amine groups. During extrusion, the MA groups of PP-g-MA are hydrolyzed to form PP-g-succinic acid, providing carboxylic acid groups for subsequent reaction in the condensation reaction.²⁸ A reduction in carboxylic acid density after extrusion would thus indicate a successful reaction between branched PEI and the MA moieties of PP-g-MA. PP-g-MA1 and PP-g-MA3 presented carboxylic acid densities of 2.41 and 12.46 nmol cm^{-2} , respectively, while all (PP-g-MAX)-g-PEIY films presented nominal carboxylic acid groups ($<0.70 \text{ nmol cm}^{-2}$), supporting that the proposed condensation reaction had occurred.

Considering the AO7 data alongside the TBO data further supports the conclusion of a successful reaction. As stated earlier, crosslinking is a possible side reaction

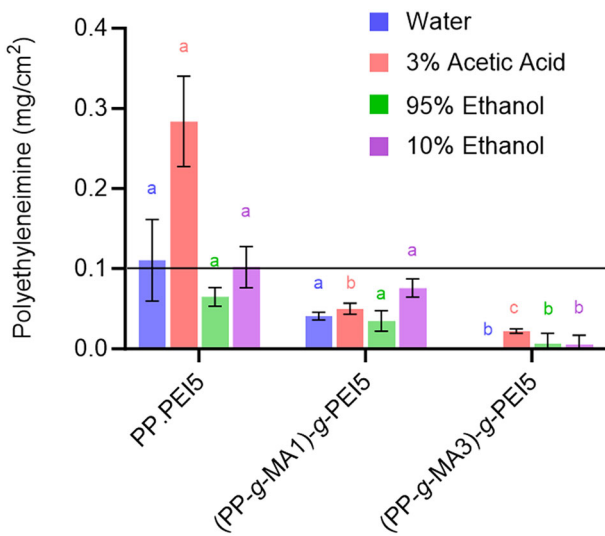


FIGURE 3 Migration of polyethyleneimine (PEI) from control and PEI grafted aminated polymer films after 10-days incubation with solvents. Results are displayed as the mean \pm the standard deviation ($n = 4$). Significant differences were calculated using a two-way ANOVA with Tukey's HSD multiple comparisons ($p < 0.05$). Significant differences are displayed for matching color-coded letters for each solvent tested. The horizontal line represents the EU limit for migration in food contact materials. ANOVA, analysis of variance; PP, polypropylene pellets. [Color figure can be viewed at wileyonlinelibrary.com]

for the current study that would result in more secondary and tertiary amines. Multiple formulations of PEI to PP-g-MA were thus tested to identify formulations, which maximize the number of surface oriented primary amines. AO7 dye assay results indicated that (PP-g-MA1)-g-PE15 and (PP-g-MA3)-g-PE15 yielded the highest density of primary amines with values of 11.96 and 7.22 nmol cm^{-2} , respectively. The lack of primary amine density reported in samples with PEI concentrations of 1% and 3% by weight (PEI1 & PEI3) suggests that at these lower concentrations of PEI, a higher degree of crosslinking across polymer chains occurred. (PP-g-MA1)-g-PE15 and (PP-g-MA3)-g-PE15 films were therefore selected for subsequent analysis.

Surface chemistry was further investigated using ATR-FTIR, as reported in Figure 2. For the PP-g-MA3 control film, the absorbance band at 1708 cm^{-1} is ascribed to C=O stretching of the carboxylic acid, while the band at 1777 cm^{-1} is attributed to the asymmetric stretching of the MA carbonyl group, which is consistent with previous reports.²⁸ Since Redfearn et al. reported that PP-g-MA films retained absorbance bands for both the anhydride and the carboxylic acid moieties post extrusion, loss or shifting of MA specific bands after reactive extrusion can be attributed to a reaction with the primary amines of PEI. (PP-g-MA1)-g-PE15 and (PP-g-

MA3)-g-PE15 had no absorbance band that could be ascribed to an anhydride peak. The band at 1702 cm^{-1} correlates to the C=O stretching of a maleimide group. The blue shift of the C=O absorbance band from PP-g-MA3 to (PP-g-MA3)-g-PE15 along with a disappearance of the anhydride peak suggests the formation of the maleimide, and a successful grafting during extrusion. Nitrogen is less electronegative than oxygen, meaning there is less of a pull on the C=O bond in a maleimide compared with anhydrides, increasing the bond's energy and frequency, shifting it to a lower wavelength. The absorbance band for the maleimide is in agreement with previous FTIR studies, where Ramesh et al. found the maleimide C=O stretching band at 1702 cm^{-1} .⁴⁷

3.3 | Nonmigratory behavior of (PP-g-MAX)-g-PE15 films

PEI has been approved by the FDA as an indirect food additive for use in polymers, paper and paper components, and adhesives⁴⁸ and has shown promise as an aminating agent in developing aminated polymers. However, its reported cytotoxicity demands that rigorous migration assays be performed to ensure its will not leach or migrate and thus be safe for use as an indirect additive in aminated polymers. To support regulatory approval of new food contact materials, there exist standardized migration assays quantifying leaching after exposure to a range of solvents designed to target conditions of intended use in contact with foods and beverages.^{35,36} While designed for food contact approval, these migration assays offer an elegant approach to support ATR-FTIR spectra indicating that the PEI was covalently bound to PP-g-MA. The nonmigratory behavior was therefore quantified using a 10-day accelerated migration assay at 40°C in four solvents of varying proticity and polarity. After incubation, the concentration of PEI in each solvent was quantified using H^1 NMR spectroscopy by comparison to a standard curve of PEI in 0.5 mL deuterium oxide. Both (PP-g-MA3)-g-PE15 and (PP-g-MA3)-g-PE15 had PEI migration levels below the EU migratory limit of 0.1 mg cm^{-2} in all four solvents tested, and presented a significant reduction in migrated PEI compared with the positive control of PEI melt blended with polypropylene without the MA copolymer (PP.PE15) (Figure 3). The notably higher migration of PEI from PP.PE15 in 3% acetic acid is likely due to protonation of the amine groups within PEI by the acid, thereby enhancing its solubility relative to other solvents. These results support the covalent nature of the grafting and the safe use of these aminated polymers.

3.4 | Radical scavenging capacity of (PP-g-MAX)-g-PEI5 films

Radical scavenging polymers have wide-ranging applications in industries in food and medicine. In food systems, oxidation can cause lipid breakdown leading to rancidity, the degradation of vitamins and nutrients, and discoloration of product,⁴⁹ leading to consumer rejection and increased food waste at the post-retail level. Similarly, antioxidant surface modifications have been researched for the medical industry to reduce oxidative stress brought on by the generation of reactive oxygen species in human cells and tissue.^{3,4} Radical scavenging activity of (PP-g-MAX)-g-PEI5 films was therefore quantified using ABTS and DPPH Trolox equivalent antioxidant assays (TEAC) to characterize radical scavenging performance in aqueous and organic environments, respectively (Figure 4). In each assay, the formation of radicals causes a colored solution, which degrades as radicals are quenched. UV-vis spectroscopy is then used to quantify the radical scavenging capacity by comparison to the Trolox standard curve. As reported in Figure 4, both (PP-g-MA1)-g-PEI5 and (PP-g-MA3)-g-PEI5 samples presented a significant increase in radical scavenging activity compared with the PP and PP-g-MAX controls in aqueous and organic systems. (PP-g-MA3)-g-PEI5 exhibited the highest radical scavenging behavior for both ABTS and DPPH with values of 5.90 and 4.31 Trolox_{eq} nmol cm⁻² respectively.

Radical scavenging activity has been previously described through three mechanisms of action: hydrogen atom transfer (HAT), single electron transfer then proton transfer (SET-PT), and sequential proton loss and electron transfer (SPLLET).⁵⁰ Each of these mechanisms depends on the protonation state of the antioxidant, and the solvent in which the assay is performed. The pKa values for PEI have been debated in literature. Many studies refer to the titration reported by Suh et al., in which 10–20% of amines are protonated at pH 7.4, while others have shown that PEI has pKa values ranging from 8.2 to 9.7.^{51,52} Since ABTS is performed at pH 7.4, most of the amines present will be deprotonated in this assay. Therefore, it is hypothesized that SPLLET is the dominant mechanism of radical scavenging for PEI. As the solvent deprotonates PEI, there is an electron transfer that would quench the free radicals for ABTS. However, since there remains a portion of amines that will be protonated, the HAT mechanism may be in part responsible for the observed radical scavenging activity. Intriguingly, the DPPH assay yielded higher antioxidant values for the PP-g-MA controls, whereas the ABTS assay exhibited increased TEAC values for the aminated samples. This distinction is attributed to enhanced interactions of PEI

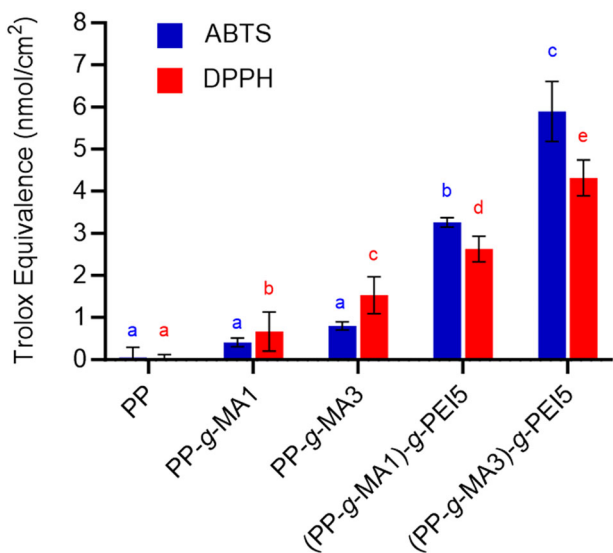


FIGURE 4 Radical scavenging capacity using two different methods. The DPPH method measures activity in the organic solvent ethanol, while ABTS is run under aqueous conditions. Results are expressed in Trolox equivalence (nmol cm⁻²) as the mean \pm standard deviation ($n = 4$). Color coded letters represent significant differences within each assay. Significant differences were calculated using a two-way ANOVA with Tukey's HSD multiple comparisons ($p < 0.05$). ANOVA, analysis of variance; PP, polypropylene pellets. [Color figure can be viewed at wileyonlinelibrary.com]

in aqueous solutions compared with ethanol. Indeed, the ionic nature of PEI promotes better solubility and increased interactions in aqueous environments compared with the organic environment of DPPH. Further studies to determine the bulk pKa of the aminated films are needed to evaluate the overall mechanism of radical scavenging. Regardless of mechanism, the results from these assays demonstrate that the aminated films have significant radical scavenging capacity that may be useful for target applications in food and medicine (Figure 4).

3.5 | Surface hydrophobicity of (PP-g-MAX)-g-PEI5 films

Dynamic water contact angle measurements were measured for amine functionalized and control films to characterize their surface wettability. Advancing water contact angle (θ_A) was performed by placing a sessile water droplet on each film's surface and recording the angle at which the baseline of the droplet starts to increase while it is expanded. Receding water contact angles (θ_R) were measured similarly, but instead measured the angle at which the baseline began to decrease while the droplet shrank. Hysteresis (θ) was then

TABLE 1 Advancing and receding water contact angles for control and active films.

Sample	Advancing (θ_A)	Receding (θ_R)	Hysteresis (θ)
PP	113.6 \pm 2.2 ^A	90.7 \pm 0.7 ^A	22.9 \pm 1.6 ^A
PP-g-MA1	110.9 \pm 4.8 ^A	56.8 \pm 3.4 ^B	53.6 \pm 6.8 ^B
PP-g-MA3	111.6 \pm 3.8 ^A	37.6 \pm 4.0 ^C	73.7 \pm 3.4 ^C
(PP-g-MA1)-g-PEI5	122.2 \pm 5.1 ^B	84.6 \pm 1.6 ^A	37.2 \pm 5.2 ^D
(PP-g-MA3)-g-PEI5	134.8 \pm 9.7 ^B	87.5 \pm 4.0 ^A	46.0 \pm 11.3 ^B

Note: Results are expressed as the mean \pm the standard deviation ($n = 6$). Letters represent significant differences between samples. Significant differences were calculated using a two-way ANOVA with Tukey's HSD multiple comparisons test ($p < 0.05$).

calculated by finding the difference of the advancing and receding water contact angles. Hysteresis can be caused by roughness on the surface or chemical heterogeneity, with a perfectly homogeneous surface having a theoretical hysteresis value of 0. Thus, in the present study, the hysteresis angles are used to indicate how homogeneous the condensation reaction occurred and can help characterize the surface chemistry of the grafted films. Results for dynamic water contact angle are reported in Table 1. All samples demonstrated advancing contact angles greater than 90°, indicating retention of the hydrophobic character of all variants despite introduction of polar primary amines in (PP-g-MAX)-g-PEI5 films. (PP-g-MA1)-g-PEI5 displayed the highest advancing water contact angle of 134.8 \pm 9.7°, nearing the superhydrophobic classification of $\geq 150^\circ$. It is interesting to observe that compared with the controls, the samples extruded with PEI both had a significant increase in advancing water contact angle. One might expect that a hydrophilic compound such as PEI would lower the contact angle due to the increased hydrogen bonding between the amines and the water droplet. This trend was also observed by Westerlind et al. where cellulose treated with PEI reduced the hydrophilic character of the fibers.⁵³ This phenomenon can be explained through the effect PEI has on the surface energy of the films. In Westerlind's paper, PEI significantly decreased the polar component of the cellulose fiber's surface energy, resulting in an increase in advancing water contact angle for the PEI treated cellulose fiber. Introduction of MA groups, increasing from control PP to PP-g-MA1 and further to PP-g-MA3 has no influence on advancing contact angle but results in a corresponding decrease in receding contact angle, a measure of the films hydrophilicity upon dewetting. The receding water contact angles for (PP-g-MA1)-g-PEI5 and (PP-g-MA3)-g-PEI5 increased to 84.6° and 87.5°, respectively, values which were not statistically different from the PP receding water contact angle.

Another explanation for the increased advancing and receding contact angles could be the miscibility of the PEI and polypropylene substrate, which is quantified through hysteresis. It has been reported that increased

miscibility (lower hysteresis) decreases interfacial surface energy, resulting in an increase in advancing and receding water contact angles. Both (PP-g-MA1)-g-PEI5 and (PP-g-MA3)-g-PEI5 exhibited a significant decrease in hysteresis (37.2° & 46.0°, respectively) compared with PP-g-MA1 & PP-g-MA3 (53.6° & 73.7° respectively), suggesting that the grafting of PEI increased the miscibility of the grafted composite blend.

3.6 | Thermal properties of (PP-g-MAX)-g-PEI5 films

Results from DSC thermograms (Table S1) provide additional insight on the observed increased water contact angles for PEI grafted films. The crystallization temperatures for (PP-g-MA1)-g-PEI5 and (PP-g-MA3)-g-PEI5 were 122.73 and 122.92°C, approximately 6 degrees higher than the controls. An increase in crystallization temperature suggests a more ordered crystalline structure. It has been reported that the introduction of a transcrystalline layer (a more ordered crystalline structure) can have significant effects on the mechanical and thermal properties of polymers.⁵⁴ PEI has previously been shown by Fang et al. to increase the total crystallization (X_c) of polypropylene composites by 33%.⁵⁵ One hypothesis is that PEI is acting as a nucleating agent to induce a transcrystalline layer in newly aminated films, which is supported by the increased thermal stability (as shown by TGA).

4 | CONCLUSION

In this work, reactive extrusion was used to amine PP-g-MA blended with polypropylene by covalently grafting PEI to the MA moieties of PP-g-MA through a condensation reaction in the melt. The grafting was confirmed by surface analysis using the TBO and AO7 dye assays along with ATR-FTIR spectroscopy. The carboxylic acid density significantly decreased from the PP-g-MA controls to the aminated samples, while the amine density increased, supporting that a reaction between the MA moieties and

primary amines occurred. The maleimide product at the grafting site is demonstrated in the ATR-FTIR spectrum through the blue shift of the C=O from 1710 cm⁻¹ in PP-g-MA3 to 1702 cm⁻¹ in the (PP-g-MA3)-g-PEI5 sample, in agreement with previous reports. The grafting reaction was further confirmed through a migration assay, where (PP-g-MA3)-g-PEI5 exhibited migration rates well below the EU migratory limit of 0.1 mg cm⁻². The new aminated films displayed active radical scavenging functionality in both aqueous and organic environments using ABTS and DPPH Trolox equivalence assays (TEAC). Based on the results from the ABTS and DPPH assays, it is hypothesized that the PEI grafted films scavenge radicals primarily via the SPLET mechanism. Dynamic water contact angle was performed to explore the wettability of the new films, where the grafting of PEI significantly increased the hydrophobic nature of the films. (PP-g-MA3)-g-PEI5 exhibited advancing water contact angle of 134.8° ± 9.7°, nearing the superhydrophobic classification of advancing water contact angles above 150°. The water contact angle results demonstrate the potential use of the new films in various applications (adhesion, packaging, self-healing materials) where hydrophobic properties are desired. Results of the present study demonstrate the use of reactive extrusion as a greener, solvent-free process to add amine functional groups to PP-g-MA compared with traditional wet chemistry methods. Since PP-g-MA itself is synthesized via reactive extrusion, our proposed approach offers the potential for a streamlined, one-step process to prepare aminated polypropylene derivatives. This reaction involves initially grafting MA onto PP, followed by the addition of PEI downstream in the extruder to be grafted onto the MA moieties. Furthermore, this reaction scheme could be used to graft PEI to other polymers with carboxylic acid functional groups such as PLA, or other amine-terminated active ligands. The versatility of the proposed reaction scheme thus opens a wide array of possible applications where amine rich polymers are desired.

AUTHOR CONTRIBUTIONS

Ian P. Kay: Conceptualization (equal); data curation (lead); formal analysis (lead); investigation (lead); methodology (lead); validation (lead); writing – original draft (lead); writing – review and editing (supporting). **Julie M. Goddard:** Conceptualization (equal); formal analysis (supporting); funding acquisition (lead); methodology (supporting); project administration (equal); resources (lead); software (lead); supervision (lead); writing – review and editing (lead).

ACKNOWLEDGMENTS

This work was supported by award number 2019-68015-29230 from the U.S. Department of Agriculture

National Institute of Food and Agriculture. This work made use of the Cornell Center for Materials Research Shared Facilities, which are supported through the NSF MRSEC program (DMR-1719875).

CONFLICT OF INTEREST STATEMENT

The authors declare no conflicts of interest.

DATA AVAILABILITY STATEMENT

Data are available on request for three years past publication.

ORCID

Julie M. Goddard  <https://orcid.org/0000-0002-3644-0732>

REFERENCES

- [1] N. Bouazizi, J. Vieillard, B. Samir, F. Le Derf, *Polymers-Basel* **2022**, *14*, 378.
- [2] Z. H. Liang, W. Rongwong, H. Liu, K. Fu, H. Gao, F. Cao, R. Zhang, T. Sema, A. Henni, K. Sumon, *Int. J. Greenhouse Gas Control* **2015**, *40*, 26.
- [3] D. Dey, M. Inayathullah, A. S. Lee, M. C. LeMieux, X. Zhang, Y. Wu, D. Nag, P. E. de Almeida, L. Han, J. Rajadas, J. C. Wu, *Biomaterials* **2011**, *32*, 4647.
- [4] J. Shi, H. Zhang, L. Wang, L. Li, H. Wang, Z. Wang, Z. Li, C. Chen, L. Hou, C. Zhang, *Biomaterials* **2013**, *34*, 251.
- [5] C. Sun, X. Feng, *Sep. Purif. Technol.* **2017**, *185*, 94.
- [6] H. Guo, T. Jiao, Q. Zhang, W. Guo, Q. Peng, X. Yan, *Nanoscale Res. Lett.* **2015**, *10*, 931.
- [7] B. Arstad, H. Fjellvåg, K. O. Kongshaug, O. Swang, R. Blom, *Adsorption* **2008**, *14*, 755.
- [8] Y. Yang, P. Qi, Y. Ding, M. F. Maitz, Z. Yang, Q. Tu, K. Xiong, Y. Leng, N. Huang, *J. Mater. Chem. B* **2015**, *3*, 72.
- [9] B. Gao, F. An, K. Liu, *Appl. Surf. Sci.* **2006**, *253*, 1946.
- [10] K. A. Gibney, I. Sovadina, A. I. Lopez, M. Urban, Z. Ridgway, G. A. Caputo, K. Kuroda, *Macromol. Biosci.* **2012**, *12*, 1279.
- [11] N. Sahiner, S. Sagbas, M. Sahiner, S. Demirci, *Polym. Degrad. Stab.* **2016**, *133*, 152.
- [12] Z. Chen, Z. Lv, Y. Sun, Z. Chi, G. Qing, *J. Mater. Chem. B* **2020**, *8*, 2951.
- [13] C. Gong, X. Zeng, C. Zhu, J. Shu, P. Xiao, H. Xu, L. Liu, J. Zhang, Q. Zeng, J. Xie, *RSC Adv.* **2016**, *6*, 106248.
- [14] R. Goyal, S. K. Tripathi, S. Tyagi, A. Sharma, K. R. Ram, D. K. Chowdhuri, Y. Shukla, P. Kumar, K. C. Gupta, *Nanomed.: Nanotechnol., Biol. Med.* **2012**, *8*, 167.
- [15] G. Moad, *Prog. Polym. Sci.* **1999**, *24*, 81.
- [16] X. Wang, C. Tzoganakis, G. L. Rempel, *J. Appl. Polym. Sci.* **1996**, *61*, 1395.
- [17] J.-M. Raquez, Y. Nabar, M. Srinivasan, B.-Y. Shin, R. Narayan, P. Dubois, *Carbohydr. Polym.* **2008**, *74*, 159.
- [18] A. A. Vaidya, I. Hussain, M. Gaugler, D. A. Smith, *Carbohydr. Polym.* **2019**, *217*, 98.
- [19] C. Liu, Z. Dai, R. Zhou, Q. Ke, C. Huang, *J. Chem.* **2019**, *2019*, 1.
- [20] M. R. Badrossamay, G. Sun, *Macromolecules* **2009**, *42*, 1948.

[21] J. Liao, N. Brosse, S. Hoppe, G. Du, X. Zhou, A. Pizzi, *Mater. Des.* **2020**, *191*, 108603.

[22] A. Létoffé, S. Hoppe, R. Lainé, N. Canilho, A. Pasc, D. Rouxel, R. J. J. Riobóo, S. Hupont, I. Royaud, M. Ponçot, *Polymer* **2019**, *179*, 121655.

[23] K. Cao, Y. Li, Z. Q. Lu, S. L. Wu, Z. H. Chen, Z. Yao, Z. M. Huang, *J. Appl. Polym. Sci.* **2011**, *121*, 3384.

[24] S. Vazquez-Rodriguez, S. Sánchez-Valdes, F. J. Rodríguez-González, M. C. González-Cantú, *Macromol. Mater. Eng.* **2007**, *292*, 1012.

[25] T. Hameed, D. K. Potter, E. Takacs, *J. Appl. Polym. Sci.* **2010**, *116*, 2285.

[26] Q. W. Lu, C. W. Macosko, J. Horrion, *J. Polym. Sci. Part a-Polym. Chem.* **2005**, *43*, 4217.

[27] J. E. Herskovitz, J. M. Goddard, *J. Agr. Food Chem.* **2020**, *68*, 2164.

[28] H. N. Redfearn, J. M. Goddard, *J. Appl. Polym. Sci.* **2022**, *139*. <https://doi.org/10.1002/app.52764>

[29] N. A. Doshna, J. E. Herskovitz, H. N. Redfearn, J. M. Goddard, *ACS Food Sci. Technol.* **2022**, *2*, 391.

[30] L. J. Bastarrachea, J. M. Goddard, *Appl. Surf. Sci.* **2016**, *378*, 479.

[31] V. P. Romani, V. G. Martins, J. M. Goddard, *Food Control* **2020**, *109*, 106946.

[32] E. Uchida, Y. Uyama, Y. Ikada, *Langmuir* **1993**, *9*, 1121.

[33] E. Kang, K. Tan, K. Kato, Y. Uyama, Y. Ikada, *Macromolecules* **1996**, *29*, 6872.

[34] Z. Lin, J. Goddard, *J. Food Sci.* **2018**, *83*, 367.

[35] FDA, Guidance for Industry: Preparation of Premarket Submissions for Food Contact Substances (Chemistry Recommendations). Nutrition, C. f. F. S. a. A., Ed.; 2007.

[36] C. Simoneau, *Guidelines on testing conditions for articles in contact with foodstuffs*, 1st ed.; Commission, E., Ed. Office for Official Publications of the European Communities, Luxembourg **2009**.

[37] J. E. Herskovitz, J. M. Goddard, *J. Appl. Polym. Sci.* **2021**, *138*, 50591.

[38] J. T. Korhonen, T. Huhtamäki, O. Ikkala, R. H. A. Ras, *Langmuir* **2013**, *29*, 3858.

[39] M. E. Hyun, S. C. Kim, *Polym. Eng. Sci.* **1988**, *28*, 743.

[40] G. Moad, *Prog. Polym. Sci.* **2011**, *36*, 218.

[41] Y. Chalamet, M. Taha, B. Vergnes, *Polym. Eng. Sci.* **2000**, *40*, 263.

[42] X. Meng, N. A. Nguyen, H. Tekinalp, E. Lara-Curzio, S. Ozcan, *ACS Sustainable Chem. Eng.* **2018**, *6*, 1289.

[43] L. Coleman, J. Bork, H. Dunn, *J. Org. Chem.* **1959**, *24*, 135.

[44] U. Schmidt, S. Zschoche, C. Werner, *J. Appl. Polym. Sci.* **2003**, *87*, 1255.

[45] I. Vermeesch, G. Groeninckx, *J. Appl. Polym. Sci.* **1994**, *53*, 1365.

[46] T. Bray, S. Damiris, A. Grace, G. Moad, M. O'Shea, E. Rizzardo, G. Van Diepen, *Macromol. Symp.* **1998**, *129*, 109.

[47] S. Ramesh, A. Sivasamy, J.-H. Kim, *Nanoscale Res. Lett.* **2012**, *7*, 350.

[48] Inventory of Food Contact Substances Listed in 21 CFR. <https://www.cfsanappsexternal.fda.gov/scripts/fdcc/?set=IndirectAdditives> (accessed).

[49] F. Tian, E. A. Decker, J. M. Goddard, *Food Funct.* **2013**, *4*, 669.

[50] I. O. Alisi, A. Uzairu, S. E. Abechi, *Helijon* **2020**, *6*, e03683.

[51] J. D. Ziebarth, Y. Wang, *Biomacromolecules* **2010**, *11*, 29.

[52] J. Suh, H. J. Paik, B. K. Hwang, *Bioorg. Chem.* **1994**, *22*, 318.

[53] B. S. Westerlind, J. C. Berg, *J. Appl. Polym. Sci.* **1988**, *36*, 523.

[54] H. Nuriel, N. Klein, G. Marom, *Compos. Sci. Technol.* **1999**, *59*, 1685.

[55] J. Fang, L. Zhang, C. Li, *Polymer* **2020**, *186*, 122025.

SUPPORTING INFORMATION

Additional supporting information can be found online in the Supporting Information section at the end of this article.

How to cite this article: I. P. Kay, J. M. Goddard, *J. Appl. Polym. Sci.* **2024**, e56085. <https://doi.org/10.1002/app.56085>